OPTO-ELECTRONICS REVIEW 8(1), 67–74 (2000)

YAG:V^{3+} – new passive Q-switch for lasers generating radiation within near infrared range

Z. MIERCZYK[1*] and Z. FRUKACZ[2]

[1]Institute of Optoelectronics, Military University of Technology
2 Kaliskiego Str., 00-908 Warsaw, Poland
[2]Institute of Electronic Materials Technology
133 Wólczyńska Str., 01-919 Warsaw, Poland

The paper presents results of investigations on growth conditions of yttrium-aluminium garnet doped with trivalent vanadium YAG:V^{3+} ions and investigations of these crystals for their application in passive Q-switches of laser resonators generating radiation within near infrared range. Absorption spectra of the crystals were examined. It was sated that within a spectral range of 720–1500 nm there are three absorption bands with their maxima for the wavelengths of 822 nm, 1098 nm, and 1282 nm. For these maxima the crystal absorption is nonlinearly dependent on intensity of incident radiation, i.e., crystal is a saturable absorber. The process of reduction of V^{5+} and V^{4+} ions to V^{3+} ones was carried out by means of crystals heating what significantly increases concentration of V^{3+} ions that are responsible for nonlinear absorption. Saturation characteristics have been determined and modulation properties in the system of YAG:Nd laser, generating giant-pulses of wavelengths of 1064 nm and 1318 nm have been investigated. Detailed review of the literature and the results of hitherto carried out investigations have been also performed.

Keywords: crystal growth, non-linear absorption, saturable absorber, giant-pulse generation.

1. Introduction

In the transmitting systems of the first laser rangefinders ruby heads (λ_{gen} = 694 nm) were used. At the end of the 60's these heads were replaced by neodymium glass lasers (λ_{gen} = 10.6 μm). At the beginning of the 70's the next generation of lasers were introduced into transmitting systems of rangefinders. They were neodymium doped ytrium-aluminium garnet – YAG:Nd^{3+} lasers (λ_{gen} = 1.064 μm). The trials of replacement of these lasers by CO_2 lasers (λ_{gen} = 1.06 μm) failed despite many advantages of the latter. At the beginning of the 90's the lasers of "eye-safe" type started to be used [1]. Spectral range of "eye-safe' laser radiation results from optical characteristics of an eye [2,3]. Main threats of eyesight caused by laser radiation relate to retina damage because cornea, lens, aqueous, and vitreous body transmit radiation of wavelengths of 400–1400 nm [4]. A laser beam is focused by eye lens on a retina where its power density and energy is of a significant value. The absorbed energy causes local heating and next radiation burn of both pigmented epithelium of retina and neighbouring photosensitive suppositories and rod cells.

This radiation burn or damage can cause permanent or temporal loss of vision in dependence on the exposure time. Radiation at wavelengths shorter than 400 nm and longer than 1400 nm is strongly absorbed by the tissues, so it does not penetrate inside an eye and does not cause retina and eye lens damage.

According to the American standard ANSI Z136.1 and the European standard EN 60 825, the wavelength of 1.5 μm is treated as a safe one for direct looking into a beam when its energy density is 100 times higher than for wavelength of 10.6 μm (CO_2 laser) and 2×10^5 times higher than for wavelength of 1.06 μm (Nd:YAG laser). It results from the estimations, based on the above-mentioned standards, that maximal giant-pulse radiation energy for 1.5 μm should not be higher than 7.9 mJ [5,6].

Two types of lasers are used in rangefinders operating within "eye-safe" range [7,8]:

- giant-pulsed Nd:YAG laser with passive Q-switching (λ_{gen} = 1.06 μm) and methane cell in which Raman shift occurs up to 1.54 μm,
- erbium giant-pulse laser with a mechanical Q-switch of a resonator (rotating prism or mirror).

Research works related to development of lasers with "eye-safe" wavelength are carried out in the following directions:

- lasers with Raman frequency shift in new media, so-called, Raman shifters [9],
- application of new active media in solid-state diode-pumped lasers or discharge lamps (YAG:Er^{3+}, YAP:Er^{3+}, YAG:Ho^{3+}, YAG:Tm^{3+}, YAG:Cr^{4+}, Er^{3+} glass) [10],

---

[*] e-mail: lastech@wat.wew.pl

- application of new media with nonlinear absorption for passive modulation of the lasers generating radiation at 1.5 µm (among others $SrF_2:Nd^{2+}$, $SrF_2:U^{4+}$, $CaF_2:U^{4+}$, $Sr_5(VO_4)_3F:Er^{3+}$, Co^{2+} doped garnets, difluorides of alkaline earth metals and U^{2+} doped glasses) [11–13].

The most promising are laser systems with erbium doped phosphate glass and passive Q-switch of resonator and the systems with conversion of a generation frequency. The above mentioned solutions which are significantly better than the lasers with gaseous high-pressure Raman's cell and erbium lasers with mechanical Q-switches will cause that the lasers generating "eye-safe" radiation will be widely applied in laser technique systems.

Figures 1 shows a spectrum of the forced Raman scattering of molecular $Ba(NO_3)_2$ crystal [14]. The dominating line is 1047.8 cm^{-1} what for YAG:Nd laser, generating radiation at 1064 nm and interaction with this medium, gives wavelengths of 1197 nm (I Stokes), 1369 nm (II Stokes), and 1598 nm (III Stokes). For the radiation at wavelength of 1.32 µm generated, among others, by YAG:Nd^{3+} and GGG:Nd^{3+} the wavelength of 1.54 µm is obtained as a results of a Raman shift.

The laser systems with frequency conversion, using $Ba(NO_3)_2$ crystals, require application of an efficient source of giant-pulses radiation at 1.32 µm because only the giant pulses can cause Raman effect in $Ba(NO_3)_2$ crystals and conversion of radiation at wavelengths of 1.32 µm and 1.54 µm with the required efficiency [15].

YAG:Nd laser (1.318 µm) with YAG:V^{3+} modulator can be a source of giant-pulses radiation at wavelength of 1.32 µm. It is reason of significant interest in YAG:V^{3+} crystal.

The undertaken research works aimed at receiving of yttrium-aluminium garnet monocrystals doped with trivalent vanadium ions (V^{3+}) and on application of this crystal for manufacturing of passive Q-switches of the lasers generating within near IR is of significant meaning for development of material base and optoelectronic components.

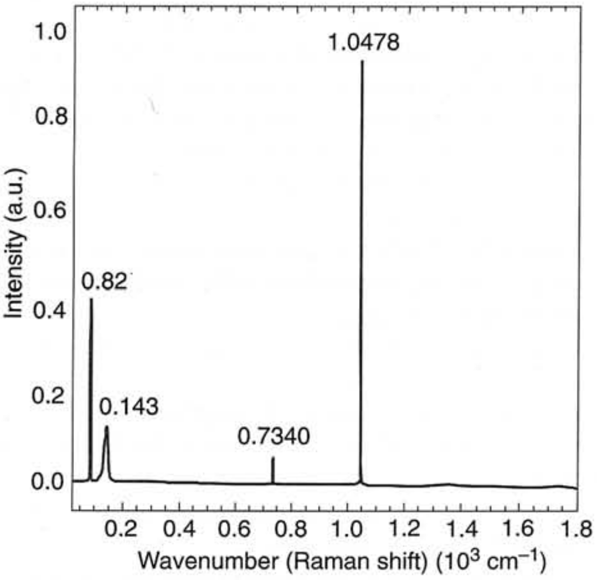

Fig. 1. Stimulated Raman scattering spectrum of $Ba(NO_3)_2$ molecular crystal (after Ref. 16).

New passive Q-switches of highly-efficient laser resonators, required for construction of laser systems and generating within "eye-safe" spectral range, are elaborated for laser devices applied in military, metrology, and automatics. Elaboration of the technology for modulators' production is an important part of research and implementation works, the goal of which is creation of new generation of laser rangefinders.

2. YAG:V^{3+} garnet

Garnet crystal lattice has cubic symmetry and spatial group O_h^{10} – Ia3d. Elementary cell consists of eight $Y_3Al_5O_{12}$ particles. In oxygen sub-lattice the following gaps are formed (lattice points): 24 dodecahedrons with the point symmetry D_2 and co-ordination 8, populated by Y^{3+}, 16 octahedrons of the symmetry C_3 and co-ordination 6, populated by Al^{3+}, and 24 tetrahedrons of the symmetry S_4 and co-ordination 4 populated also by Al^{3+}. Garnet doping consists in substitution of dopant atoms to one or more cation centre. It was stated that vanadium atoms substitute only Al^{3+} in octahedral and tetrahedral centres [17,18]. A matrix, i.e., a lattice of pure YAG garnet, is optically neutral in the range from ultraviolet to far infrared, so all optical effects of doped garnet are dependent on dopants properties and ligand fields symmetry.

Optical properties – a spectrum of absorption of vanadium ions doped YAG crystals were examined for the first time in 1971 by Weber and Riseberg [19]. They stated that in the absorption spectrum within the range of 300–1400 nm there are four bands of significantly different intensity that were classified according to valency number (valence) of emitting ion and its position in a lattice. The results of these investigations are listed in Table 1.

In a lattice of garnet crystal, vanadium can have all its valencies V^{5+}, V^{4+}, V^{3+}, and V^{2+}. As it can be seen in Table 1, in the registered spectra, only the band originating from V^{3+} and V^{4+} ions has been found. V^{5+} ion is isoelectron ion with argon atom ($V^{5+}:1s^22s^2p^63s^2p^6$) and it does not show optical activity. V^{2+} ions are placed in main dodecahedral points because of their large sizes and, as it results from theory, they show insignificant absorption and emission abilities but their spectra are quenched or masked by intense, wide bands of V^{3+} and V^{4+} ions.

The second stage of YAG:V^{3+} investigations were those undertaken by Russian and Belorussian researches. The results of their investigations are published in Refs. 17,18, 20–22. The most important result of these works was a discovery that this crystal is a saturable absorber and that V^{3+} ions have such property in tetrahedral points, i.e., according to Weber and Riseberg [19] the band of 1250 nm. It means that this crystal can be used as passive Q-switch for

Table 1. Substantial spectroscopic properties of YAG crystals doped with vanadium ions.

No.	Vanadium valence	Co-ordinating polyhedron	Band maximum (nm)	Band width (nm)	Band intensity (a.u.)
1	3+	Octahedron	425	350–480	1
2	3+	Octahedron	615	550–700	0.5
3	3+	Octahedron	975	–	Invisible
4	4+	Tetrahedron	~ 800	650–900	0.07
5	4+ (V) 2+ (Ca)	Tetrahedron Dodecahedron	700 800	600–900	2.6
6	3+	Tetrahedron	1250	1050–1450	0.02

the lasers emitting in this band. It was experimentally stated that modulation occur for the wavelength of 1340 nm (YAP:Nd laser), 1064 nm (YAG:Nd laser), 780 nm (Al_2O_3:Ti laser), and 747 nm (YAP:Pr laser). So, if saturable absorption is also in 800 nm band [19], this band is a superposition of the bands formed by V^{4+} and V^{3+} being in tetrahedral points.

Figure 2 presents a diagram of energetic levels of V^{3+} in tetrahedral points. It results from a diagram that there are possible the following quantum transitions from a ground state (GSA)

$$^3A_2 \rightarrow {}^3T_1(^3P), \quad {}^3A_2 \rightarrow {}^3T_1(^3F).$$

Moreover, there are possible the following transitions from the excited state (ESA)

$$^1E(^1D) \rightarrow {}^1T_1(^1G) \text{ and } {}^1E(^1D) \rightarrow {}^1E_1(^1G)$$

These transitions can influence modulation properties of YAG:V^{3+} crystal.

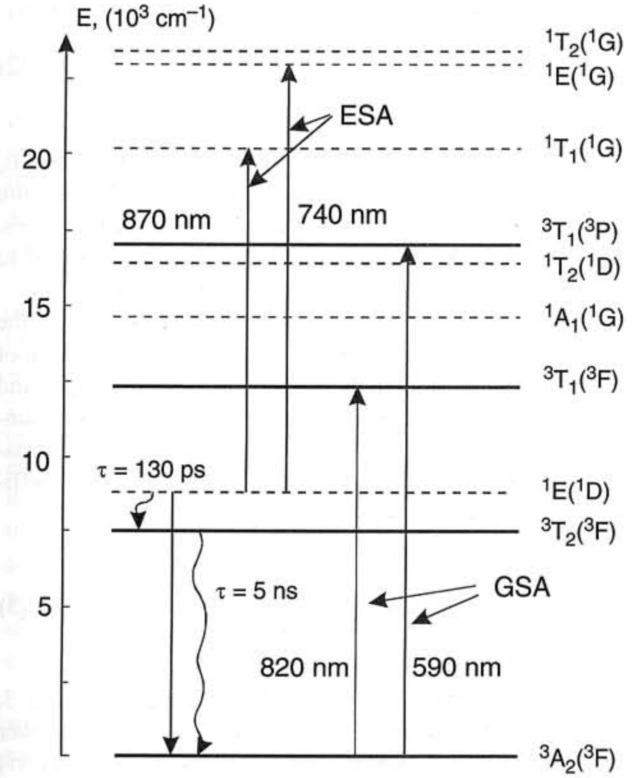

Fig. 2. Scheme of energy level for tetrahedral V^{3+} ions in YAG crystal lattice (after Ref. 23).

Quantum transitions from the ground state (GSA) and transitions from the excited states (ESA) are denoted in Fig. 2.

The authors do not inform about quality of the crystals in view of their applications in laser technology. Concentration of vanadium ions is determined as $n = 2 \times 10^{20}$ cm^{-3} and it is vanadium concentration of crystallisation starting composition or vanadium concentration in a crystal [19,20]. Information on V^{3+} ions concentration in tetrahedral positions are given indirectly as absorption cross-section for wavelength of 1.08 µm $\sigma = (8.2 \pm 2.5) \times 10^{-18}$ cm^2 and for wavelength of 1.33 µm $\sigma = (1.7 \pm 0.5) \times 10^{-17}$ cm^2.

The crystals were obtained using gradient freeze method (GFM).

3. Crystal growth

The crystals were obtained by the Czochralski method using iridium crucible of external dimensions ϕ50×50×1.5 mm. As the parent substance, high purity oxides were used: Y_2O_3(5N) and Al_2O_3(5N) J.M.&Prod., V_2O_3(3N) Aldrich.

Two charges, placed in a crucible were prepared, the first one with vanadium pentoxide V_2O_5 and the second one with V_2O_3. In both charges the amount of vanadium oxide was so chosen to have concentration of vanadium atoms equal to 0.7%. The percentage of vanadium atoms was calculated in relation to the number of lattice points, populated by aluminium atoms, i.e., for the total amount of octahedral and tetrahedral points. It was stated that distribution of vanadium atoms between both types of the lattice points will be statistical distribution but not necessary proportional to their number; among all the points populated by aluminium 3/5 are octahedrons and 2/5 are tetrahedrons.

Because the melting temperature of V_2O_5 is 690°C and the charge synthesis reaches the melting temperature of 1970°C, this oxide should be handled with care and the activities aimed at protection of V_2O_5 evaporation should be undertaken.

The crystallisation processes were carried out in nitrogen atmosphere with small amount of oxygen (percentage fraction). For preparation of the crystallisation processes and two kinds of charges; first with V_2O_5 and second one with V_2O_3, the below-presented processes of crystal growth with possibly high concentration of V^{3+} ions were assumed.

In the first case we introduce large amount of "bad" V^{5+} ion into a crystal. However, this ion of smaller ion radius (0.56 Å), comparable with ion radius Al^{3+}, has higher chances to take smaller tetrahedral point. Reduction of V^{5+} to V^{3+} will occur in solid phase during heating process and with no necessity to change position in a crystal lattice.

In the second case "good" but large size V^{3+} ion (0.96 Å) will take rather octahedral points, so tetrahedral points will be taken by Al^{3+}. In such a situation heating causes rather diffusive change of the points of V^{3+} and Al^{3+} ions what is significantly less efficient and it will be much more difficult to have good crystal with the expected configuration of ions.

Four processes were carried out, two of each charge and four light-green crystals of a diameter of 16–18 mm with no rod were obtained. Each successive second crystal was pulled from a material remaining in a crucible after the first crystal growth and it was supplemented with the mass of primary charge which was equal to the mass of pulled crystal with no consideration for dopant segregation.

Pulling the larger number of crystals with the method of a charge completion was too risky because there was small but clear evaporation of vanadium oxide (V_2O_5) from a crucible what appears as a deposit on the elements of crystallisation chamber. Moreover, a characteristic phenomenon occurs; each the first crystal grows in cylindrical form, straight in [111] direction but each next crystal shows tendency to helical growth. A deviation from [111] direction was observed and lateral plates of growth disappeared. Despite these effects the crystals had good optical properties and fulfilled predicted expectations.

In the crystallisation process, as a result of introduction of vanadium atom dopants into $Y_3Al_5O_{12}$ structure, V^{3+} ion substitutes Al^{3+} in octahedral points or tetrahedral ones. During crystal growth only a small number of vanadium atoms penetrate into a crystal structure as V^{3+} ions in tetrahedral positions but remaining atoms are at different positions or at the higher state, i.e., V^{4+} and V^{5+} [19].

Vanadium ions of V^{3+} valence being in the required points of a YAG structure can be obtained as a result of complex reactions in a solid phase that proceed in the process of multi-stage heating of a crystal kept in vacuum and reducing atmosphere.

The aim of the work was to obtain YAG:V^{3+} crystals having significantly higher concentration of V^{3+} ions than "as grown" concentration in tetrahedral positions. For this purpose there was applied the method of thermal treatment of a crystal in reducing atmosphere, called also crystal heating.

4. Non-linear absorption

Absorption of radiation during its transmission through the medium is characterised by an absorption coefficient describing decrease in radiation intensity. If intensity of a plane wave is equal to I(z), its attenuation after transmission through the medium layer of the thickness dz equals

$$dl = -kIdz \tag{1}$$

The linear absorption coefficient k is equal to the fraction of radiation intensity dI/I, absorbed in the layer of the thickness dz = 1 cm.

The value of absorption coefficient depends on electrons structure and a symmetry of the initial state E_i and the final state E_k of particles transition that are characterised by the populations N_i and N_k as well as the statistic wages g_i and g_k. It is often convenient to express probability of the absorption cross section σ_{ik} determining radiation absorption by one particle. It is connected with an absorption coefficient by the following relation

$$k_{ik} = \sigma_{ik}\left(N_i - N_k \frac{g_i}{g_k}\right) \tag{2}$$

Until the populations N_i and N_k of the levels E_i and E_k are not noticeably modified, as a result of interaction with radiation field, they can be considered as the constant ones. Intensity of the absorbed radiation is then proportional to intensity of the incident light (linear absorption).

For the higher intensities I, the population N_i of the lower state E_i can significantly decrease and population of the upper state N_k can increase. The values of $N_i(I)$ and $N_k(I)$ are now the functions of I and as a result dI is no longer proportional to I (non-linear absorption). With increasing intensity of the incident beam I, the absorption coefficient for two-level system

$$k = \frac{k_0}{1+S} = \frac{k_0}{1+I/I_s} \tag{3}$$

approaches zero for I → ∞. This case is illustrated in Fig. 3.

A phenomenon of non-linear absorption (absorber bleaching) is used in laser technology to shape temporal characteristics of laser radiation, mainly in order to generate giant pulses by means of passive Q-switch.

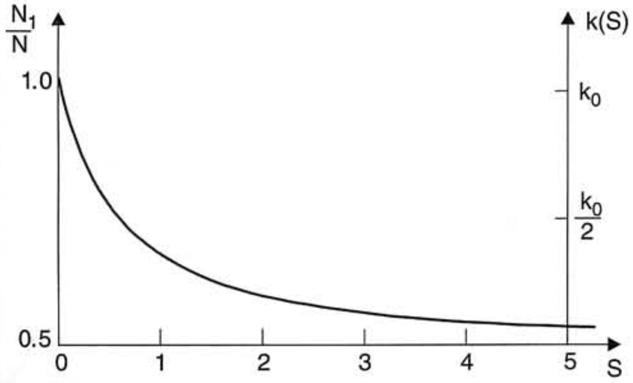

Fig. 3. The ratio N_1/N ($N = N_1 + N_2$) and the absorption coefficient k for two-level system as a functions of the saturation parameter S (after Ref. 24).

In a laser system with non-linear absorber (Q-switch), the output absorption coefficient (for low intensities) should be so chosen to avoid generation of pulsed laser during increase in population inversion of amplifying medium. Just after pump actuation, during initial phase of laser action generation does not occur.

During this time increasing spontaneous emission is absorbed by an absorber, lowering its absorption, what causes increase in the flux of photons travelling along the axis what next accelerates absorption decrease and so on. The number of photons rises and more and more absorber atoms are in the excited state and as a result total absorption decreases and radiation intensity continuously increases and finally saturation state is obtained. Then, the absorber has optimal transmission close to 1 and the resonator has minimal losses – Q-switch is open.

This phenomenon would not be repeated if a relaxation time of an absorber would be significantly longer than pumping pulse duration. In fact, the relaxation times used for absorbers are $\tau = 10^{-6}$–10^{-12} s so, after the time τ the absorber's atoms return to the ground state and the same they can absorb radiation again.

The process starts from the beginning, so the second pulses or even further pulses with a sufficient energy can be produced. In order to produce the only one giant pulse, an initial absorption should be so high that the produced energy will not be sufficiently high for the second switch opening. Because opening of the switch depends on temporal course of absorption and it is determined by intensity of the existing radiation field, the opening time is comparable (of the same order of magnitude) with the laser excitation time. Moreover, for the relaxation times that are of the same order of magnitude as the period of pulse transmission through the resonator or even shorter ones, the pulse can be repeatedly transmitted through the switch.

The first media applied in laser technology that showed non-linear absorption were dyes characterising by wide absorption lines. Thus, accurate resonance of absorption band with a laser line is not essential. It is important to have a dye with any absorption with saturation effect for laser line.

The structure of energetic levels of absorbing centres in real systems of non-linear absorbers, i.e., glasses, crystals, ceramics or semiconductors is complex and results from quantum processes proceeding in an absorber. This structure is usually modelled by means of two-, three-, or four-level quantum systems while each of the considered electron levels can have oscillating structure [25,26].

5. Results of spectroscopic investigations and their interpretation

In order to carry out spectral measurements, the plane-parallel plates of a thickness of about 1 mm were cut from the obtained crystals and next grinded and polished. The measurements were made within the spectral range of 200–1100 nm using the Perkin Elmer Lambda-2 spectrophotometer and within 1100–1500 nm using Beckman Acta MVII spectrometer but within 1.5–25 µm using the Perkin Elmer FTIR 1725 spectrometer. On the basis of the measurements of the samples transmission T(λ), the absorption coefficient was calculated with consideration of multiple reflections of radiation inside a sample. Figure 4 shows the calculated absorption spectrum of the investigated "as grown" crystals within the range of 200–5800 nm Fig. 4(a) and 300–1500 nm Fig. 4(b).

In the absorption spectra of "as grown" crystals the following bands can be distinguished:

A – within the range of 300–500 nm (max for 426 nm) related to the transitions in V^{3+} ion in octahedral position (co-ordination 6),

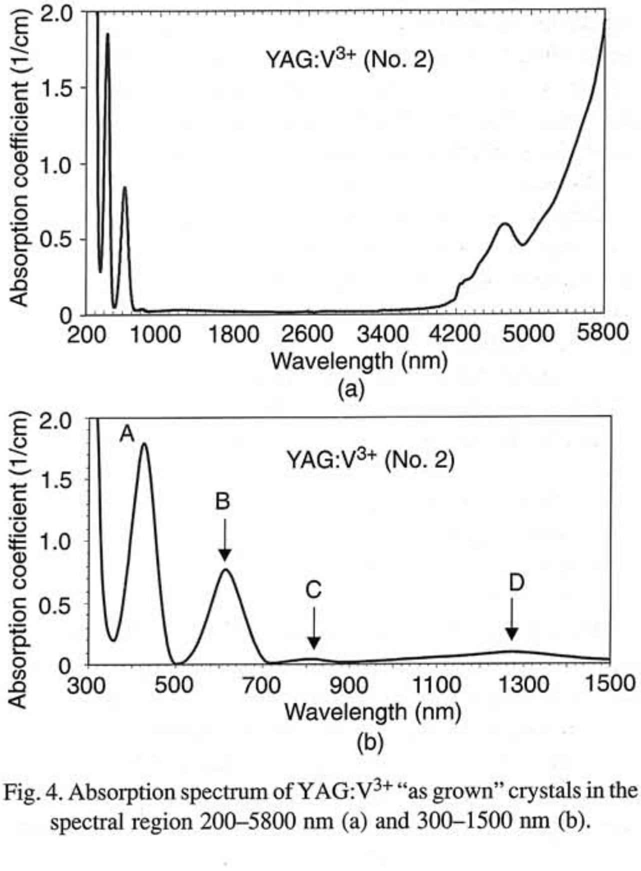

Fig. 4. Absorption spectrum of YAG:V^{3+} "as grown" crystals in the spectral region 200–5800 nm (a) and 300–1500 nm (b).

- B – within the range of 500–720 nm (max for 625 nm) related to the transitions in V^{3+} ion in octahedral position,
- C – within the range of 720–900 nm (max for 822 nm) related to the transitions in V^{3+} ion in tetrahedral position (co-ordination 4),
- D – within the range of 900–1500 nm originating from V^{3+} ions in tetrahedral position with two maxima 1098 nm and 1282 nm.

The C and D bands are characteristic for YAG:V^{3+}. In this spectral range the crystal has phototropic properties.

All the investigated samples taken from the all obtained crystals show similar spectral character. Only slight differences in band intensities have been observed. No absorption was stated out in the presented spectrum range, only natural matrix absorption [pure YAG – see Fig. 4(a)] could be seen. In a spectrum, all bands occur which existence have been already described in other works [17,23]. In order to make the spectrum description clear we denote the bands by the letters or wavelengths of their maxima; A – 426 nm, B – 625 nm, C – 822 nm, D – 1098/1282 nm.

The bands C and D in near IR are interested for us and they have low intensity for "as grown" crystals what is caused by small number of V^{3+} ions in tetrahedral points and this crystal is useless for practical application.

The "as grown" YAG:V^{3+} crystals, obtained with the Czochralski method were next subjected to thermal treatment in reducing atmosphere.

Figure 5 presents typical changes in absorption spectrum of the crystal after the successive stages of a heating process. It results from the obtained results of the investigated samples that this process influences the raise of concentration of V^{3+} ions in tetrahedral positions. There is observed significant increase in absorption coefficient in all the bands (Fig. 5). Also the shift of maxima of B and C bands, in relation to the spectrum of "as grown" crystals can be seen.

Increasing ions number (concentration) $n(V^{3+})$ in a crystal causes increase in the absorption coefficient k. The relationship is described by the formula $k_\lambda = n(V^{3+})\sigma_\lambda$ where σ_λ is the collision cross section of an absorption for the wavelength λ.

Assuming for the band maximum D $\sigma \approx 10^{-18}$ cm^2 [9], we have concentration of V^{3+} ions in the crystals, characterised by the curves 1, 2, and 3, respectively:

$n_1(V^{3+}) \approx 2.5\times10^{17}$ cm^{-3},
$n_2(V^{3+}) \approx 6\times10^{17}$ cm^{-3},
$n_3(V^{3+}) \approx 1.5\times10^{18}$ cm^{-3}.

During the processes of thermo-chemical treatment, the number of V^{3+} ions significantly increases and there occurs their advantageous redistribution in a crystal what can be seen in Fig. 5. In these processes the number of V^{3+} ions increases but also due to optically inactive V^{5+} ions the number of V^{4+} ions increases, too. The analysis of absorption curves carried out in the further part of this paper testifies about the fact that many V^{5+} ions are in the crystal, independently of using of V_2O_5 or V_3O_3 as a charge material.

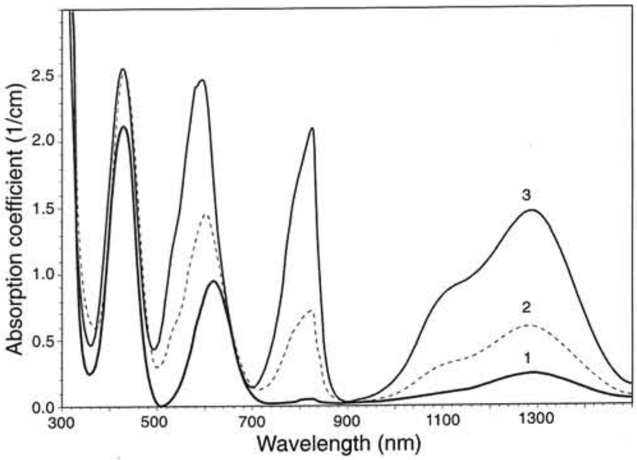

Fig. 5. Three absorption curves present three stages of crystal "improvement"; 1 – "as grown" crystal, 2 and 3 – two thermo-reduction processes in a solid phase.

The shape of the charts of the bands B, C, and D indicates that each of them is superposition of at least two Gaussian curves. The method of Gaussian distribution was used for curve 3 of Fig. 5. The experimental curve k(λ) was approximated by the sum of the Gaussian curves

$$k(\lambda) = \sum_i k_i^{\max} \exp\left(- \frac{4 \ln 2(\lambda - \lambda_i^{\max})^2}{(\Delta\lambda_i)^2} \right)$$

where i is the number of absorption bands, $k_i^{\max}$ is the maximal value of the i_{th} band, $\lambda_i^{\max}$ is the maximal position of the i_{th} band, $\Delta\lambda_i$ is the half-width of the i_{th} band, while the distribution coefficients $(k_i^{\max}, \lambda_i^{\max}, \Delta\lambda_i)$ were determined numerically using non-linear optimisation, i.e., minimising the squares sum of deviations of approximating curve from experimental one.

The distribution effect presents Fig. 6. Complex character of absorption spectrum is shown what makes its interpretation easier. The band A (426 nm) has Gaussian shape and it is a simple band generated by octahedral ions V^{3+} [18]. The band B is a superposition of the three bands: B_1, B_2, and B_3. The band B_1 (535 nm), B_2 (590 nm) is generated by V^{3+} ion in tetrahedral position and it corresponds to the transition of $^3A_2 \rightarrow {}^3T_1(^3P)$, the band B_3 (625 nm) is generated by octahedral V^{3+} ion. The band D consists of D_1(1098 nm) and D_2(1282 nm) bands. These bands are generated by tetrahedral V^{3+} ion and correspond to $^3A_2 \rightarrow {}^1E(^1D)$ and $^3A_2 \rightarrow {}^3T_2(^3F)$ transitions, respectively.

Complex character of the spectra and presence of the bands originating from V^{3+} ions in the bands B, C, and D can be observed for high concentration of these ions in a crystal. Weber and Risberg [19] do not have such crystals. Even using a compensator (Ca^{2+} ions), the bands originating from V^{3+} ions in tetrahedral positions, within the

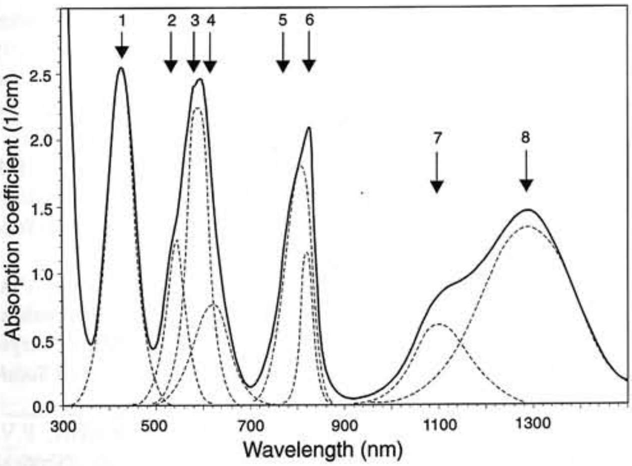

Fig. 6. Approximation of absorption curve of YAG: V^{3+} crystal by a sum of the Gaussian curves, 1 – 426 nm, 2 – 530 nm, 3 – 590 nm, 4 – 625 nm, 5 – 780 nm, 6 – 822 nm, 7 – 1098 nm, 8 – 1282 nm.

range of 625 nm and 800 nm, could not appear on the background of the intense octahedral V^{3+} bands and tetrahedral V^{4+} band.

6. Laser investigations – results and discussion

Investigations of properties of spectroscopic absorbers YAG:V^{3+} with various concentration of V^{3+} ions were carried out on the basis of analysis of bleaching dynamics. The changes of transmission of the investigated samples were determined as a function of power density of the transmitted radiation, emitted by giant-pulse YAG:Nd laser (30 mJ, 6 ns) and tunable Al_2O_3:Ti laser pumped with the second harmonics of YAG:Nd. A tunable Al_2O_3:Ti laser used for measurements makes it possible to choose a generation line of 822 nm with an accuracy of ±0.3 nm. This laser generated the radiation monopulses of energy of 8 mJ and pulse duration of 10 ns at the line of 822 nm. A power density of diagnostic pulse was changed within the range of 5–800 MW/cm^2.

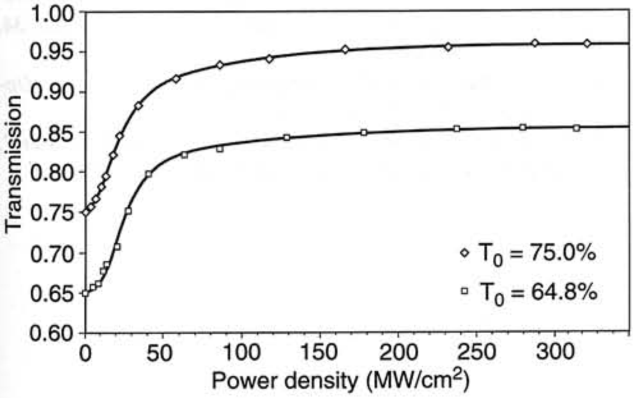

Fig. 7. Transmission changes of examined YAG:V^{3+} samples with various V^{3+} ions concentration and under infulence of giant-pulse laser radiation of 1064 nm.

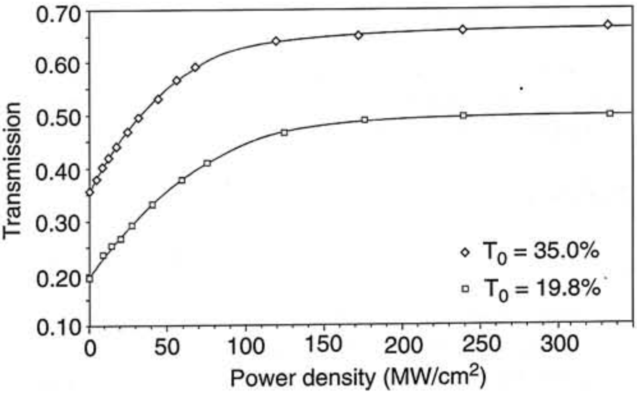

Fig. 8. Transmission changes of examined YAG:V^{3+} samples with various V^{3+} ions concentration and under influence of giant-pulse laser radiation of 822 nm.

Figure 7 presents the results of measurement of the transmission changes in two samples YAG:V^{3+}, with initial transmission of 64.8% and 75.0%, as a function of power density of laser radiation at wavelength of 1064 nm (YAG:Nd). Figure 8 shows the results of measurement of transmission changes of two samples YAG:V^{3+}, with initial transmission of 19.8% and 35.2%, as a function of power density of laser radiation at wavelength 822 nm (Al_2O_3:Ti).

The inactive losses, absorption cross-section, concentration of active centres, relaxation time, and energy losses for absorber bleaching, i.e., the parameters required for analysis and optimisation of Q-switched giant-pulse laser were estimated on the basis of two-level quantum model of an absorber [27,28].

In the system with YAG:Nd laser (1064 nm) and YAG:V^{3+} modulator having the initial transmission T_o(1064 nm) = 55% there have been produced the giant pulses, duration of which was 20 ns and the initial energy 5 mJ but in YAG:Nd laser system (1318 nm) with YAG:V^{3+} modulator having the initial transmission T_o(1318 nm) = 58% there has been produced the giant-pulses, duration of which was 30 ns and the output energy 4 mJ.

7. Conclusions

The YAG:V^{3+} crystals with V^{3+} ions concentration of about 1.5×10^{18} cm^{-3} have been obtained. These crystals show non-linear absorption in three bands with their maxima at 822 nm, 1098 nm, and 1282 nm. Bleaching effect has been investigated for wavelength of laser emission at 822 nm (Al_2O_3:Ti) and 1064 nm (YAG:Nd). The Q-switched passive modulators made of YAG:V^{3+} crystals were applied in two resonator systems of YAG:Nd laser and generation of monopulse radiation at wavelengths of 1064 nm and 1318 nm was obtained.

Advantageous spectroscopic parameters of YAG:V^{3+} crystals and characteristic for garnets high thermal and mechanical resistivities, makes it possible to apply this crystal in laser technology as a material for Q-switched passive modulators of laser resonators generating in near IR.

Acknowledgements

The investigations have been carried out within the scope of grants No 0 T00A 004 13 and No 7 T08A 020 13, financed by the State Committee for Scientific Research.

References

1. R. Pengelley, "OEC's eye-safe laser option", *Int. Defense Review* **2**, 1990.
2. L.K. Matthews and G.V. Garcia, *Laser and Eye Safety in the Laboratory*, SPIE Press PM19, 1994.
3. W.J. Geeraets and E.R. Berry, "Ocular spectral characteristics as related to hazards from lasers and other light sources", *Am. Jour. of Ophthalmology* **61**, 15–20 (1968).
4. D.H. Sliney, "Selected papers on laser safety", *SPIE Milestone Series*, **MS-117**, Bellingham, Washington, 1995.
5. IEC Standard EN 825-1, "Safety of laser product. Equipment classification, requirements and user's guide", 1993.
6. ANSI Z-136.1-1993, "American national standard for the safe use of lasers", 1993.
7. *Laser Rangefinders*, JANE's Armour and Artillery Upgrades, Eleventh edition 1998-99, Jane's Information Group Ltd., Couldson, Surrey UK, 1998.
8. E. Gregor, D.E. Nieuwsma, and R.D. Stultz, "20 Hz eye-safe laser rangefinder for air defence", *Proc. SPIE* **1207**, 124–134 (1990).
9. Z. Mierczyk, "New materials for coherent pumped laser systems. Active mediums, frequency conversion systems and non-linear elements", *Proc. SPIE* **3186**, 22–23 (1997).
10. S. Jiang, J. Myers, D. Rhonehouse, M. Myers, R. Belford, and S. Hamlin, *Laser and Thermal Performance of a New Erbium Doped Phosphate Glass*, Ed. Kigre, Inc. Hilton Head Island, 1990.
11. R.D. Stultz, M.B. Camargo, and M. Birnbaum, "Divalent uranium and cobalt saturable absorber Q-switches at 1.5 µm", *OSA Proc. on Advanced Solid-State Lasers* **24**, 460–464 (1995).
12. Y. Jiang, R. Wu, D.L. Rhonehouse, M.J. Myers, J.D. Myers, and S.J. Hamlin, "Bleaching and Q-switching of U^{2+}:CaF_2 at 1535 nm", *Proc. SPIE* **2379**, 1–6 (1995).
13. R.E. Peale, H. Weidner, and W.A. McClintic, "Er^{3+}: $Sr_5(VO_4)_3F$: A potential passive Q-switch for Er-glass lasers", *OSA Proc. on Advanced Solid-State Lasers* **24**, 519–522 (1995).
14. J.T. Murray, R.C. Powell, N. Peyghambarian, D. Smith, W. Austin, and R.A. Stolzenberg, "Generation of 1.5 µm radiation through intracavity solid state Raman shifting in $Ba(NO_3)_2$ nonlinear crystals", *Optics Lett.* **20**, 1017–1019 (1995).
15. V.B. Sigachev, T.T. Basiev, M.E. Doroshenko, V.V. Osiko, and A.G. Papashvili, "1.3 µm neodymium lasers passively Q-switched with Nd^{2+}:SrF_2 and YAG:V^{3+} crystals and Raman shifting to eye-safe region", *OSA Proc. on Advanced Solid-State Lasers* **24**, 454–459 (1995).
16. P.G. Zverev, T.T. Basiev, J.T. Murray, R.C. Powell, R.J. Reeves, "Stimulated Raman scattering of picosecond pulses in $Ba(NO_3)_2$ crystals", *OSA Proc. on Advanced Solid-State Lasers* **15**, 156–160 (1993).
17. V.P. Mikhailov, N.I. Zhavoronkov, N.V. Kuleshov, V.A. Sandulenko, K.V. Yumashev, and P.V. Prokoshin, "Mode-locking of near infrared lasers with YAG:V^{3+} crystal as a saturable absorber", *OSA Proc. on Advanced Solid-State Lasers* **15**, 354–358 (1993).
18. V.P. Mikhailov, N.V. Kuleshov, N.I. Zhavoronkov, P.V. Prokoshin, K.V. Yumashev, and V.A. Sandulenko, "Optical absorption and nonlinear transmission of tetrahedral V^{3+} (d_2) in yttrium aluminium garnet", *Optical Materials* **2**, 267–272 (1993).
19. M.J. Weber and L.A. Riseberg, "Optical spectra in yttrium aluminium garnet", *J. Chemical Physics* **55**, 2032–2038 (1971).
20. L.J. Krutova, N.A. Kulagin, and V.A. Sandulenko, "Absorption and luminescence spectra of octahedral and tetrahedral V^{3+} ions in garnets", *Proc. of the IX Symposium on Spectroscopy of Crystals Doped with R-E and TM*, Leningrad, 81 (1990).
21. A.S. Grenishin, W.M. Kisieler, and L.J. Krutova, *Proc. of Intern. Conf. Laser Optics 93*, St. Petersburg, 248 (1993).
22. V.P. Mikhailow and N.J. Zhavoronkov, *Proc. of Intern. Conf. Laser Optics 93*, St. Petersburg, 247 (1993).
23. V.G. Shcherbitsky, N.N. Prosnov, V.P. Mikhailow, and V.A. Sandulenko, "Ultrafast dynamics of excited-state absorption in YAG:V^{3+} crystal", *J. Appl. Phys.* **80**, 4782 (1996).
24. V.P. Mikhailov, K.V. Yumashev, N.V. Kuleshov, A.M. Malyarevich, V.G. Shcherbitsy, P.V. Prokoshin, and N.N. Posnov, "Ultrafast dynamics of excited-state absorption in YAG:V^{3+}", *OSA TOPS on Advanced Solid-State Lasers* **1**, 591–594 (1996).
25. W. Demtröder, *Laser Spectroscopy*, 2nd edition, Springer-Verlag, Berlin/Heidelberg, 1998.
26. F. Gan, *Laser Materials*, World Scientific Publishing Co., Singapore, London, 1995.
27. W. Rudolph and H. Weber, "Analysis of saturable absorbers, interacting with Gaussian pulses", *Optics Commun.* **34**, 491–496 (1980).
28. M. Hercher, "An analysis of saturable absorbers", *Appl. Optics* **6**, 947–954 (1980).
29. J.J. Degnan, "Optimisation of passively Q-switched lasers", *IEEE J. Quantum Electronics* **31**, 1890–1901 (1995).